Research Article Adv. Mater. Lett. 2015, **6**(10), 913-919 Advanced Materials *Letters*

www.amlett.com, www.vbripress.com/aml, DOI: 10.5185/amlett.2015.5931 Published online by the VBRI Press in 2015

Biophysical study on the interaction of spirooxindole-annulated thiopyran derivatives with bovine serum albumin using spectroscopic and docking methods

Swarup Roy[1], Sudipta Ponra[2], Raj Kumar Nandi[2], K. C. Majumdar[2*], Tapan Kumar Das[1*]

[1]*Department of Biochemistry and Biophysics, University of Kalyani, Kalyani 741235, West Bengal, India*
[2]*Department of Chemistry, University of Kalyani, Kalyani 741235, West Bengal, India*

[*]Corresponding author. Tel: (+91) 3473-238373 (R); E-mail: tapankumardas175@gmail.com (T.K. Das), Tel: (+91) 33-2582 7521 (R); E-mail: kcmklyuniv@gmail.com (K.C. Majumdar)

Received: 01 April 2015, Revised: 28 May 2015 and Accepted: 26 June 2015

ABSTRACT

The study of interaction between spirooxindole-annulated thiopyran derivatives (STP) and bovine serum albumin (BSA) was investigated using multi-spectroscopic and docking method. The intrinsic fluorescence of BSA could effectively quenched by STP through dynamic quenching. The thermodynamic parameters suggested that hydrogen bonds and van der Waals forces played a key role in stabilizing the BSA–STP complexes. According to Forster non radiation energy transfer theory (FRET) the average binding distance (r) between STP and BSA were found to be < 7 nm. Furthermore, UV-visible and circular dichroism results indicated that in presence of STP secondary structure of BSA changed. Theoretical docking study of the interaction of BSA and STP also supported the experimental results. Copyright © 2015 VBRI Press.

Keywords: Bovine serum albumin; thiopyran; spectroscopy; CD; docking.

Introduction

The study of interactions between biomolecules and synthetic organic compounds has evoked increasing research interest at present. The binding of small molecules with serum albumin is very significantly as the properties like absorption, distribution, metabolism, excretion, stability and toxicity can be changed due to the binding of small molecules [**1**]. Furthermore, it has been showed previously that the conformation of serum albumin is altered upon binding with chemicals and this reflects in the secondary and tertiary structure of serum albumins as well as in their biological function [**2–4**]. Bovine and human serum albumins show approximately 76 % sequence homology [**5**]. Due to the medical importance, low-priced, ready availableness, and strange ligand-binding properties BSA is frequently used as a protein model in related study [**6**]. Among the important heterocyclic systems indole ring is the structural framework in a many bioactive natural products and pharmaceuticals [**7**]. Although, the chemistry of thiopyran has been less explored but still substantial biological activities related with the sulfur-heterocyclic scaffolds have been identified. The anti-bacterial, [**8**] anti-hyperplasia, [**9**] analgesic, and anti-cancer [**10, 11**] activities are some activities shown by thiopyran and fused-thiopyran derivatives. Indole subunits are also common heterocyclic system in large number of bio-active natural products [**12-15**]. Therefore, thiopyrano indole-annulated heterocyclic compounds which are a combination of biologically important indole and thiopyran units are very important for biological studies. Spectroscopic approaches are often applied to reveal the accessibility of quenchers to albumin's fluorophore groups, help understand albumin's binding mechanism to small molecules, and provide information about the nature of binding phenomenon **[16-18]**.

In the featured work, we desired to demonstrate the interaction between STP and BSA by spectroscopy. Spirooxindole-annulated thiopyran derivatives have already been synthesized [**19**]. The objective of our study was to determine the affinity of STP to BSA and investigation of thermodynamics of BSA-STP interaction. We used UV-Vis, fluorescence, and circular dichroism spectra to investigate the binding of STP and BSA. According to FRET the energy transfer between BSA and STP was studied. Furthermore, employment of molecular modeling was made to understand the theoretical interaction of STP derivatives with BSA.

Experimental

The spirooxindole-annulated thiopyran derivatives required for our study were prepared according to published procedure [**19**] as shown below (**Scheme 1**).

Bovine Serum Albumin (Sigma) was used in this experiment. The solution of BSA was prepared by dissolving BSA in a Tris-HCl (50 mM, pH 7.4) buffer to make the concentration as 1 µM. Synthesized STP (1 mM) was dissolved in methanol. All the other chemicals were of analytical reagent grade and double distilled water was used throughout the course of this study.

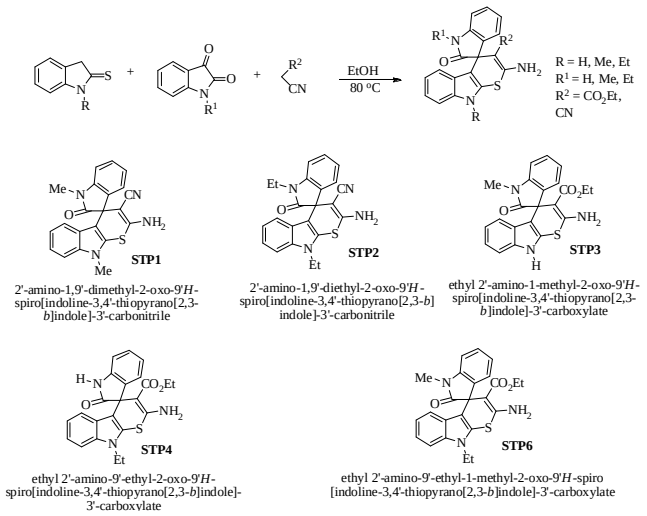

Scheme 1. Various synthesized spirooxindole-annulated thiopyran derivatives.

Fluorescence spectra were recorded on a Cary-Eclipse fluorescence spectrophotometer (Agilent Technologies) well equipped with Cary temperature controller. The absorption spectra were obtained from a Cary 100 UV-Vis spectrophotometer (Agilent Technologies). Circular dichroism was recorded in a Jasco J-815 CD spectrometer.

The absorption titration experiments were performed keeping BSA (1 µM) concentration fixed while changing the STP concentration (0 to 30 µM). The absorption spectra were recorded from 230 to 330 nm at room temperature (303 K). All the experiments were carried out in Tris-HCl (50 mM, pH 7.4) buffer in a conventional quartz cell.

BSA solution (1 µM) was titrated by successive additions of (0 to 20 µM) STP. Fluorescence spectra were recorded in the range of 300-450 nm at the excitation wavelength of 279 nm. The fluorescence spectra were also studied at 293, 303, and 313 K. The range of synchronous scanning were λex = 240, λem (a) = 255, λem (b) =300 nm, where the differences in the wavelengths (Δλ) were 15 and 60 nm respectively.

The far-UV CD region (190–260) was analyzed to give the content of the regular secondary structure in BSA. Protein solutions were prepared in Tris-HCl (50 mM, pH 7.4) buffer. Protein solutions of 0.04 µM were used to obtain the spectra. Spectral changes of BSA were monitored after adding different concentration of STP (0 to 50 µM).

The crystal structure of BSA was accessed from the Protein Data Bank (PDBID: 4F5S). The Auto Dock 4.0 was used to calculate the possible binding mode of the STP with BSA. The 3-D structure of STP and BSA were docked employing molecular modeling software and then analyzed by Discovery digital studio 4.0. The docking computation was then executed using the Lamarckian genetic algorithm (LGA) for ligand conformational searching. To estimate the possible binding conformations of STP, LGA was used in the Auto dock. Now, a maximum of 10 different conformations were considered during the docking process and among all the conformer with the lowest binding free energy was utilized for further analysis.

Results and discussion

Absorption characteristics of BSA-STP interaction

The intensity at the wavelength of BSA increases with increasing addition of STP1 [**20**] **(Fig. 1)**. The values of the apparent association constant (K_{app}) were obtained from the BSA absorption as described previously [**20, 21**]. Now, the values of K_{app} were estimated using linear reciprocal plots based on following Eq. (1) [**22**].

$$\frac{1}{A_{obs}-A_0}=\frac{1}{A_C-A_0}+\frac{1}{K_{app}(A_C-A_0)[STP]} \quad (1)$$

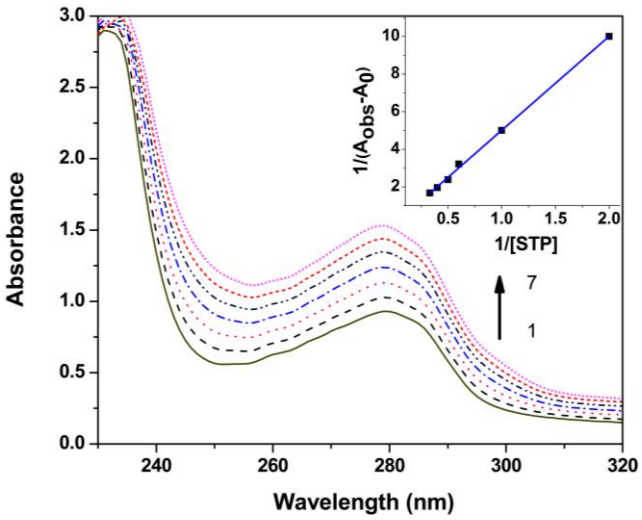

Fig. 1. (Color online) Absorption spectra of BSA (1 µM) in presence of STP1 (1-7): (0 to 30 µM), inset showing calculation of Kapp of BSA–STP complex; $1/(A_ob_s-A_0)$ vs 1/[STP] plot.

where, A_0 is the absorbance of BSA in the absence of STP and A_C is the recorded absorbance at 279 nm for BSA at different STP concentrations. The plot of $1/(A_ob_s-A_0)$ vs 1/[STP] is linear and Kapp was estimated to be 2.8×10^2 L/mol (R= 0.9993, where R is the correlation coefficient) (**Fig. 1 inset**) [**26**]. The value of small value of K_{app} indicating formation of a weak complex between STP1 and BSA. In case of STP2, STP3, STP4 and STP6; K_{app} values are 3.69×10^3, 6.02×10^3, 4.57×10^3, and 9.26×10^2 L/mol respectively, results are given in **supplementary materials** [**S1**] (R= 0.9997, 0.9968, 0.9985, and 0.9948 for STP2, STP3, STP4 and STP6 respectively). The values of K_{app} are considerably small, which suggested the formation of a weak complex between BSA and STP.

Characteristics of fluorescence spectra

It is observed in **Fig. 2** that with the increase addition of STP1 the emission intensity of BSA gradually diminishes with red shift of emission wavelength. This observation suggested that STP can strongly interact with BSA and

quench its intrinsic fluorescence. The observed result is consistent with that of the absorption spectra. The quenching properties can be explained using Stern-Volmer equation (Eq. 2) [**24, 25**].

$$F_0 / F = 1 + K_q \tau_0 [Q] = 1 + K_{SV}[Q] \quad (2)$$

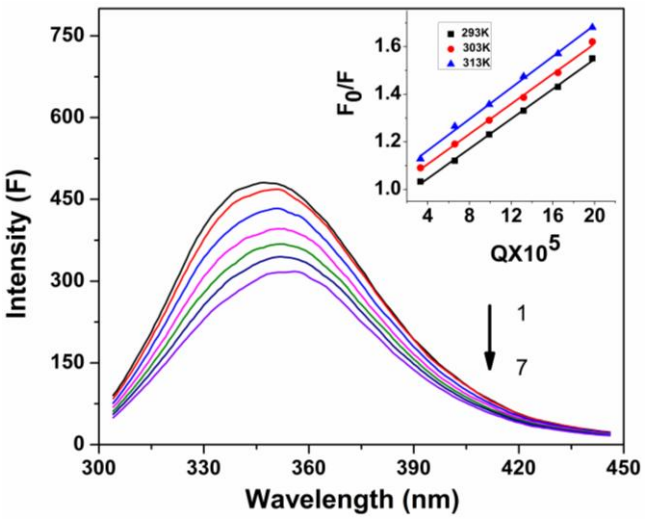

Fig. 2. (Color online) Fluorescence quenching spectra of BSA by STP1, λex= 279 nm; C (BSA) =1μM; C (STP) (1-7): (0, 3.3, 6.6, 9.9, 13.2, 16.5, and 19.8 μM respectively), inset showing Stern Volmer plot for STP and BSA at 293, 303, and 313 K, respectively.

where, F_0 and F are the fluorescence intensities in the absence and presence of a quencher, K_q is the bimolecular quenching constant, K_{SV} is the Stern Volmer constant, τ_0 is the average lifetime of the molecule in the absence of a quencher and [Q] is the concentration of the quencher (STP). Since the fluorescence lifetime of a biopolymer is 10^{-8} s [**24**], the Kq values are estimated by this relation- $K_q = K_{SV}/\tau_o$. The maximum scatter quenching collision constant of various quenchers with the biopolymer for dynamic quenching is near 1×10^{10} L/mol/s [**24**]. Quenching data can be evaluated as plots of F_0/F vs [Q]. A plot of F_0/F vs [Q] yields a slope equal to Stern Volmer quenching constant. The values of K_{SV} and K_q at varying temperatures are shown in **Table 1**. The linearity of the F_0/F vs [Q] plots is shown in **Fig. 2 inset**. As mentioned in **Table 1**, the K_q increases with the increase of temperature (293-313K), this suggests that possible quenching mechanism is a dynamic quenching process. From **Table 1**, it is observed that the binding constant of the interaction between STP and BSA increases in the following order: STP1 < STP2 < STP4 < STP3 < STP6 indicating that STP6 has the highest ability to quench BSA fluorescence and compound STP1 is the weakest to quench BSA. Figure of emission spectra and Stern Volmer plot STP2, STP3, STP4 and STP6 are given in supplementary materials.

Binding constant (K) and number of binding sites (n)

The data of fluorescence intensities were analyzed by using Eq. 3. The number of binding sites (n) and the binding constant (K) were estimated using the Eq. 3 [**26-28**].

$$\log \frac{F_o - F}{F} = \log K + n \log[Q] \quad (3)$$

A plot of log [(F_0−F)/F] vs log [Q] gives a linear plot and **Fig. 3** presents the double logarithm plots. The values of 'n' (**Table 2**) at the experimental temperatures are almost equal to one that shows that there is a single binding site in BSA for STP and the value is dependent of temperature (293-313 K).

Table 1. The Stern-Volmer constants, and quenching constants of BSA by STP at varying temperatures.

Compound	Temperature (K)	K_{SV} (L/mol) ×10²	K_q (L/mol/S)×10⁻⁶	R[a]
STP1	293	3.13	3.13	0.9992
STP2	293	4.92	4.92	0.9963
STP3	293	5.45	5.45	0.9991
STP4	293	5.19	5.19	0.9935
STP6	293	6.07	6.07	0.9979
STP1	303	3.16	3.16	0.9987
STP2	303	5.18	5.18	0.9988
STP3	303	5.47	5.47	0.9980
STP4	303	5.99	5.99	0.9969
STP6	303	6.67	6.67	0.9990
STP1	313	3.29	3.29	0.9987
STP2	313	5.60	5.60	0.9985
STP3	313	5.60	5.60	0.9964
STP4	313	6.15	6.15	0.9965
STP6	313	6.66	6.66	0.9986

[a] correlation coefficient.

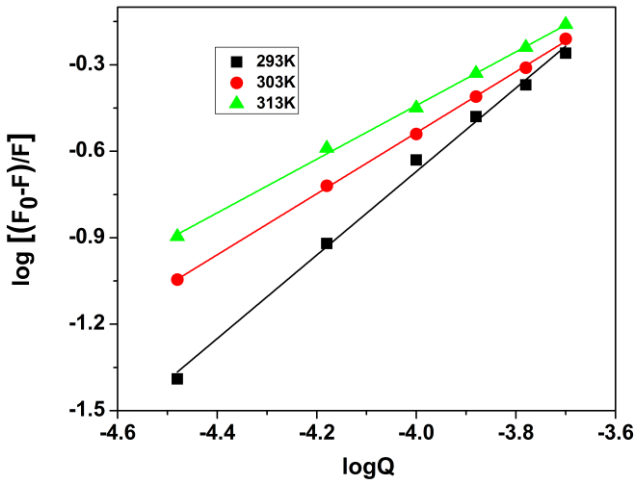

Fig. 3. (Color online) Plots of the STP1quenching effect on BSA fluorescence at varying temperature (293, 303, 313 K).

From **Table 2**, it is observed that the binding constant of the interaction between STP and BSA increases in the following order: STP2 < STP6 < STP3 < STP4 < STP1 i.e., STP1 has the strongest ability to bind with BSA and STP2 is the weakest. With the rise of temperature the binding constant K decreases suggesting that the stability of the STP-BSA complexes is lowered with rise of temperature.

Thermodynamic parameters and nature of binding forces

The possible interactive forces between biomolecules and small molecules are hydrogen bonding, van der Waals, hydrophobic and hydrophilic and electrostatic interactions. If enthalpy change (ΔH) does not largely vary over the

temperature range studied, then ΔH and entropy change (ΔS) are determined using the Van't Hoff Eq. (Eq. 4), where K is the binding constant at the corresponding temperature (**Fig. 4**).

Table 2. Binding constants (K) and number of binding sites (n) of BSA by STP at varying temperatures.

Compound	Temperature (K)	K (L/mol)	n	R[a]
STP1	293	5.01×10^{11}	1.45	0.9979
STP2	293	3.16×10^{10}	1.26	0.9981
STP3	293	7.94×10^{10}	1.28	0.9995
STP4	293	3.16×10^{11}	1.36	0.9996
STP6	293	3.98×10^{10}	1.22	0.9994
STP1	303	3.31×10^{8}	1.06	0.9998
STP2	303	1.25×10^{9}	1.06	0.9995
STP3	303	3.16×10^{9}	1.11	0.9992
STP4	303	7.94×10^{9}	1.14	0.9988
STP6	303	1.25×10^{10}	1.17	0.9995
STP1	313	2.3×10^{7}	0.93	0.9992
STP2	313	1.12×10^{8}	0.93	0.9995
STP3	313	6.30×10^{8}	1.04	0.9991
STP4	313	1.25×10^{9}	1.08	0.9991
STP6	313	1.0×10^{9}	1.02	0.9974

[a]Correlation coefficient.

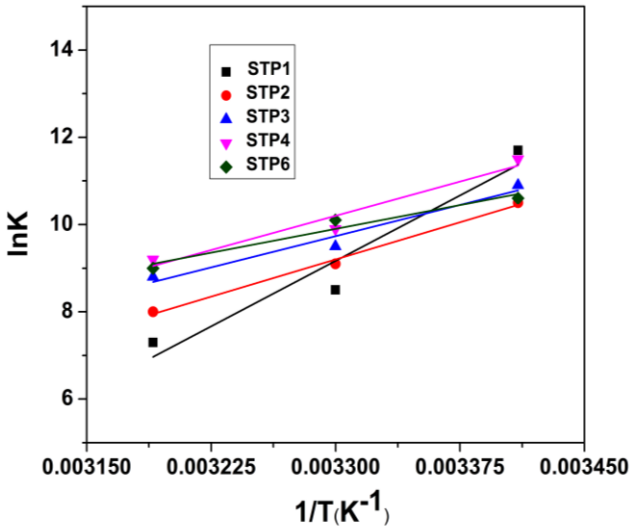

Fig. 4. (Color online) The Van't Hoff plot for the interaction of BSA and STP derivatives.

$$\ln K = -\Delta H / RT + \Delta S / R \quad (4)$$

The Gibbs free energy change (ΔG) is calculated from the eq. 5.

$$\Delta G = \Delta H - T\Delta S = -RT \ln K \quad (5)$$

According to the enthalpy and entropy changes, the model of interaction is –ΔH > 0 and ΔS > 0: indication of hydrophobic forces; ΔH < 0 and ΔS < 0: indication of van der Waals interactions and hydrogen bonds; ΔH≈0 and ΔS>0: indication of electrostatic interactions [**23, 27-29**].

Table 3 shows (supplementary information) the values of ΔH and ΔS obtained from **Eq. 4**. The values of ΔH and ΔS are found to be -166.28 kJ/mol and -472.48 J/mol/K respectively in case of STP1. In case of STP2, STP3, STP4 and STP6, respectively similar results were observed (**S1**); all the values of thermodynamic parameters are given in **Table 3 (supplementary file)**. As shown in **Table 3**; all the values of ΔG, ΔS, and ΔH are found to be negative. The negative value of ΔG revealed that the interaction process was spontaneous. Accordingly, negative value of ΔS and ΔH suggests that weak forces like van der Walls and hydrogen bonding are predominant in this binding process [**30**].

Synchronous fluorescence spectra

Synchronous fluorescence spectroscopy is used to analyze the micro-environmental changes of chromospheres [**31**]. The value of Δλ i.e. difference between excitation and emission wavelengths is an important parameter. According to Miller [**32**] when Δλ=15 nm, synchronous fluorescence spectra provides information on the microenvironment of tyrosine residues and when Δλ=60 nm, it provides information on the microenvironment of tryptophan residues. In **Fig. 5b (supplementary file)**, when Δλ=60 nm there is a no shift of the emission wavelength of tryptophan residues and when Δλ= 15 nm, (**Fig. 5a, supplementary file**) there is a slight blue shift of the emission wavelength of tyrosine. The slight blue shift of the emission maxima of tyrosine suggests the polarity around the tyrosine residues is decreased and the hydrophobicity is increased in the presence of STP1 [**33**]. These results suggested that STP1 induces a very small conformational change in BSA. In case of STP2, STP3, STP4 and STP6 respectively almost same type of results were observed given in **supplementary materials** (**S1**).

Circular dichroism spectroscopy

Circular dichroism is commonly used for the determination of secondary structure of protein molecules [**34**]. The CD spectrum of BSA exhibited two negative minima at 208 nm and 222 nm [**26**]. **Fig. 6** (**supplementary file**) shows the helicity of BSA in the presence of increasing concentration of STP. The CD results are expressed in terms of mean residue ellipticity (MRE) in deg cm^2 $dmol^{-1}$ according to the following eq. [**35**],

$$MRE = \frac{obsCD(m\deg)}{Cp \times n \times l \times 10} \quad (6)$$

Here, Cp is the molar concentration of the protein, n is the number of amino acid residues and l is the path length. The α-helical contents (%) were estimated from MRE values at 208 nm using the eq. [**36**],

$$\alpha - helix(\%) = \frac{-MRE_{208} - 4000}{33000 - 4000} \times 100 \quad (7)$$

Here, MRE_{208} is the observed MRE value at 208 nm, 4000 is the MRE of the β-form and random coil conformation cross at 208 nm and 33000 is the MRE value of a pure α-helix at 208 nm. From Eq. (6) and (7), the -helicity in the secondary structure of BSA can be estimated. According to the above equation the % α -helix of BSA was estimated and it showed that the percentage of helicity of

BSA is 47.20 % in pure BSA. In the presence of STP1 % α -helix of BSA decreases to 44.60 % and 43.34 % in the presence of 25µM and 50 µM STP1 respectively. The result indicates the loss of α-helix due to the interaction of STP with BSA. The reduction of percentage of protein α-helix structure indicates that STP bound with the amino acid residue of the main polypeptide chain of BSA leading in the decrease of hydrogen bonding network. That is structure of BSA is altered in the presence of STP1 [**37**] i.e., interaction of STP1 with BSA causes some conformational change. In STP2, STP3, STP4 and STP6 with BSA also showed similar result given in **supplementary materials (S1)**.

Energy transfer between BSA and STP derivatives

Energy transfer between small molecules and biomolecules generally can be classified into two types: radiative energy transfer and non-radiative energy transfer. The non-radiative type can be explained by FRET. FRET is frequently used to calculate the distance between amino acid residues on proteins and drugs in the binding sites, under the following three conditions (a) the donor can produce fluorescence; (b) the absorption spectrum of the receptor overlaps sufficiently with the donor's fluorescence emission spectrum and (c) the distance between donor and acceptor is less than 7 nm.

According to FRET [**38**], the efficiency of energy transfer (E) and the distance (r) of binding between BSA and STP can be calculated by the following equation.

$$E = 1 - \frac{F}{F_o} = R_0^6 / (R_0^6 + r^6) \quad (8)$$

Here, F and F_o are the fluorescence intensities of BSA in the presence and absence of STP, r is the distance between acceptor and donor and R_o is the critical distance when the transfer efficiency is 50 %, Ro can be calculated from the following equation 9.

$$R_0^6 = 8.8 \times 10^{-25} k^2 N^{-4} \phi J \quad (9)$$

Here, k^2 is the spatial orientation factor between the emission dipole of the donor and the absorption dipole of the acceptor. Theoretically k^2 can range from 0 to 4, but very rigid conformations are necessary for the extreme values. If both the donor and acceptor are tumble rapidly free to assume any orientation and, k^2 equals 2/3. N is the refractive index of the medium, ϕ is the fluorescence quantum yield of the donor and J is the overlap integral of the fluorescence emission spectrum of the donor and the absorption spectrum of the acceptor. J is given by the following equation.

$$J = \sum F(\lambda)\varepsilon(\lambda)\lambda^4 \Delta\lambda / \sum F(\lambda)\Delta\lambda \quad (10)$$

where, F (λ) is the fluorescence intensity of the fluorescent donor at wavelength λ and it is dimensionless; ε (λ) is the molar absorption coefficient of the acceptor at wavelength λ. J can be calculated by integrating the spectra as presented in **Fig. 7** (**supplementary**).

It has been described for biomolecules, k^2 = 2/3, ϕ = 0.15 and N = 1.336 [**39**]. The experimental results are shown in **Table 4** (**supplementary file**). In case of STP2, STP3, STP4 and STP6, respectively similar results were obtained, given in **supplementary materials** (**S1**). The average distances between a donor fluorophore and acceptor fluorophore on the 2–7 nm scale [**40, 41**] denotes that the energy transfer occurs between BSA and STP [**42, 43**] and the fluorescence quenching of BSA is non-radiative transfer process.

Molecular modeling

Molecular modeling was performed by docking STP to BSA to determine the preferred binding site and the binding mode. Molecular docking technique has been applied to understand different binding modes of BSA–STP interaction [**44, 45**]. The 3D structure of BSA was collected from Proteins Data Bank. The possible conformations of the BSA–STP complex were calculated using Auto dock 4.0 program. The most appropriate energy ranked model (**Fig. 8a**) revealed that the bound at the interface between two sub domains IIA and IIIA, which are located just above the entrance of the binding pocket of IIA.

STP1 molecule is surrounded by11 amino acid residues within 5Å: 5 hydrophobic residues (ILeu141, Leu115, Pro113, Pro117, Ile181), 2 hydrophilic residues (Tyr160, Tyr137) and 4 ionic residues (Arg185, Arg144, Glu182, Lys114). What is more, there are three hydrogen bonds between the hydroxyl groups of SPT1 and the amino acid residues of BSA; they are Chain A: Arg185:NH1:B-:Lig1O, Lig1:N-A:Leu115:O and Lig1:N-A:Glu182:O (**Fig. 8b**).

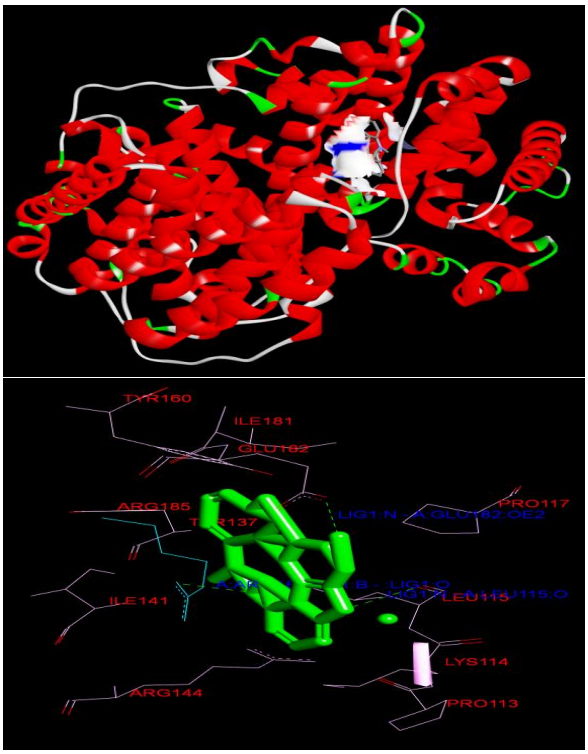

Fig. 8. (Color online) Conformation for STP docked to BSA, a) place of interaction of STP1 and BSA and b) The surrounding amino acid residues of BSA within 5 Å from STP (green colored).

In case of STP2, STP3, STP4 and STP6, respectively similar results were observed and given in **supplementary materials** (**S1**).The formation of hydrogen bonds decreases the hydrophilicity and increases the hydrophobicity to stabilize the BSA-STP system. Therefore, it is concluded that the interaction between STP and BSA is dominated by hydrogen bonds and van der Wall's interactions which are in well agreement with the results of experimental binding mode study.

Conclusion

We investigated the interaction of STP with BSA by spectroscopic and docking study. Result indicative of dynamic quenching process. The binding reaction is spontaneous and van der Waals interactions and hydrogen bonding play a key role. The synchronous fluorescence and CD spectra suggest that the conformation of BSA is subjected to alteration in the presence of STP. The binding distance of STP1 with BSA was calculated to be 3.64 nm, on the basis of the Förster's theory and results indicates that the energy transfer can occur with ease. Moreover, molecular docking study supports the interaction between the STP and BSA and the finding is consistent with the available reported data.

Acknowledgements
SR is thankful to the Department of Science and Technology (New Delhi, India) for a DST INSPIRE fellowship (IF110421). S.P and R.K.N thank CSIR (New Delhi) for their research fellowships. KCM thanks UGC (New Delhi) for Emeritus Fellowship.

Author contributions
Conceived the plan: SR; Performed the expeirments: SR; Data analysis: SR; Wrote the paper: SR, TKD, SP, RKN, KCM (SR, TKD, SP, RKN, KCM are the initials of authors). Authors have no competing financial interests.

Supporting information
Supporting informations are freely available from VBRI press.

Reference

1. Neelam, S.; Gokara, M.; Sudhamalla, B.; Amooru, D.G.; Subramanyam, R., **2010**, *114*, 3005. **DOI:** 10.1021/jp910156k
2. Varlan A.; Hillebrand, M.; *Molecules*, **2010**, *15*, 3905. **DOI:** 10.3390/molecules15063905
3. Solomonov A.V.; Rumyantsev E. V.; Ivanov S. P.; Kochergin B. A.; Antina, E.V.; *Protein J*, **2013**, *32*, 343. **DOI:** 10.1007/s10930-013-9493-2
4. Timerbaev A. R.; Hartinger C. G.; Aleksenko S. S.; *Chem. Rev.*, **2006**, *106*, 2224. **DOI:** 10.1021/cr040704h
5. Leslie C.; Scott , C. J. W.; Cair, F. I., *Med. Lab. Sci*., **1992**, *49*, 319. **ISSN:** 0308-3616
6. Xiao, C. Q., Jiang, F. L.; Zhou, B.; Li, R.; Liu, Y.; *Photochem. Photobiol. Sci.*, **2011**, *10*, 1110. **DOI:** 10.1039/C1PP05008G
7. Vine, K. L.; Matesic, L.; Locke, J. M.; Ranson, M.; Skropeta, D.; Cytotoxic and anticancer activities of isatin and its derivatives: a comprehensive review from 2000-2008, *Anti-Cancer Agents Med. Chem.*, **2009**, *9*, 397. **ISSN:** 1875-5992
8. Brown, M. J.; Carter, P. S.; Fenwick, A. E.; Fosberry, A. P.; Hamprecht, D. W.; Hibbs, M. J.; Jarvest, R. L.; Mensah, L.; Milner, P. H.; Hanlon, P. J. O.; Pope, A. J.; Richardson, C. M.; West, A.; Witty D. R.; *Bioorg. Med. Chem. Lett*., **2002**, *12*, 3171. **ISSN:** 0960-894X
9. Quaglia, W.; Pigini, M.; Piergentili, A.; Giannella, M.; Gentili, F.; Marucci, G.; Carrieri, A.; Carotti,; Poggesi, A. E.; Leonardi, A.; Melchiorre, C. J.; *J. Med. Chem.* **2002**, *45*, 1633. **DOI:** 10.1021/jm011066n
10. Berlin, K. D.; Benbrook, D. M.; Nelson, E. C.; Administering heterocyclic ethers or sulfides to induce apoptosis, cell differentiation and as anti-carcinogenic agents, U.S. Patent 6586460, **2003**.
11. Sugita, Y.; Hosoya, H.; Terasawa, K.; Yokoe, I.; Fujisawa, S.; Sakagami, H.; Cytotoxic Activity of Benzothiepins against Human Oral Tumor Cell Lines, *Anticancer Res*., **2001**, *21*, 2629.
12. Carle, J. S.; Christophersen, C. J.; *J. Org. Chem*., **1980**, *45*, 1586. **DOI:** 10.1021/jo01297a007
13. Ohmoto, T.; Koike, K.; *Chem. Pharm. Bull*., **1984**, *32*, 170. **DOI:** 10.1248/cpb.32.170
14. Taniguchi, M.; Anjiki, T.; Nakagawa, M.; Hino, T.; *Chem. Pharm. Bull*., **1984**, *32*, 2544. **DOI:** 10.1248/cpb.32.2544
15. Kamijo, S.; Yamamoto, Y. J.; *J. Org. Chem*., **2003**, *68*, 4764. **DOI:** 10.1021/jo034254p.
16. Guo, X. J.; Hao, A. J.; Han, X. W.; Kang, P. L.; Jiang, Y. C.; Zhang, X. J.; *Mol. Biol. Rep*., **2011**, *38*, 4185.
17. Zhang, G.W.; Zhao, N.; Wang, L.; *J. Lumin*., **2011**, *131*, 880. **DOI:**10.1016/j.jlumin.2010.12.018
18. Brockhinke, A.; Plessow, R.; Kohse-Höinghaus, K.; Herrmann, C.; *Phys. Chem. Chem. Phys.*, **2003**, *5*, 3498. **DOI:** 10.1039/B303262K
19. Majumdar, K. C.; Ponra, S.; Nandi, R. K.; *Tetrahedron Letters*, **2012**, *53*, 1732. **DOI:** 10.1016/j.tetlet.2012.01.099
20. Mariam, J.; Dongre, P. M.; Kothari, D. C.; *J. Fluorescence*, **2011**, *21*, 2193. **DOI:** 10.1007/s10895-011-0922-3.
21. Stephanos, J. J.; *J. Inorg. Biochem*., **1996**, *62*, 155. **ISSN:** 0162-0134
22. Marty, R.; Nsoukpoe-Kossi, N. C.; Charbonneau, D.; Weinert, C. M.; Kreplak, L.; Tajmir-Riahi, H. A.; *Nucleic Acids Res*., **2009**, *37*, 849. **DOI:** 10.1093/nar/gkn1003
23. Roy, S.; Das, T. K.; *J. Nanosci. Nanotechnol*. **2014**, *14*, 4899. **DOI:** 10.1166/jnn.2014.9508
24. Lakowicz, J. R.; 3rd edn, Principle of fluorescence spectroscopy, Springer, New York, **1999**. **DOI:** 10.1007/978-0-387-46312-4
25. Wang, R.; Chai, Y.; Wang, R.; Zhang, L.; Wu, J.; Chang, J.; *Spectrochimica Acta A*: **2012**, *96*, 324. **DOI:** 10.1016/j.saa.2012.05.030
26. Kandagal, P. B.; Ashoka,S.; Seetharamappa, J.; Shaikh, S. M. T.; Jadegoud, Y.; Ijare, O. B.; *J Pharm. Biomed. Anal*., **2006**, *41*, 393. **DOI:** 10.1016/j.jpba.2005.11.037
27. Roy, S.; Das, T. K.; *Nanosci. Nanotechnol. Lett.*, **2014**, *6*, 547. **DOI:** 10.1166/nnl.2014.1852
28. Roy, S.; Sadhukhan, R.; Ghosh, U.; Das, T. K.; *Spectrochimica Acta Part A*, **2015**, *141*, 176. **DOI:** 10.1016/j.saa.2015.01.041
29. Ross, P. D.; Subramanian, S.; *Biochemistry*, **1981**, *20*, 3096. **DOI:** 10.1021/bi00514a017
30. Roy, S.; Das, T. K.; *Adv. Sci Eng. Med*., **2014**, *6*, 1105. **DOI:** 10.1166/asem.2014.1617
31. Hu, Y.-J.; Liu, Y.; Pi, Z.-B.; Qu, S.-S.; *Bioorg. Med. Chem*. **2005**, *13*, 6609. **DOI:** 10.1016/j.bmc.2005.07.039
32. Miller, J. N.; Recent advances in molecular luminescence analysis, *Proc Anal Div Chem Soc*., **1979**, *16*, 203.
33. Zhong, Y.; Zhou, B.; Liu, Y.; Zhou, C.; Ding, X.; Liu, Y.; *J. Fluoresc*., **2008**, *18*, 109. **DOI:** 10.1007/s10895-007-0247-4
34. Kelly, S. M.; Tess, T. J.; Price, N. C.; *Biochim. Biophys. Acta*, **2005**, *1751*, 119. **DOI:** 10.1016/j.bbapap.2005.06.005
35. Bi, S.; Song, D.; Tian, Y.; Zhou, X.; Liu, Z.; Zhang, H.;*Spectrochim. Acta A*, **2005**, *61*, 629. **DOI:** 10.1016/j.saa.2004.05.028
36. Cheng, X. X.; Liu, Y.; Zhou, B.; Xiao, X.H.; Liu, Y.; *Spectrochim. Acta A*, **2009**, *72*, 922. DOI: 10.1016/j.saa.2008.12.003
37. Kang, J.; Liu, Y.; Xia Xie, M.; Li, S.; Jiang, M.; Wang, Y.D.; *Biochim. Biophys. Acta*, **2004,** *1674*, 205.

DOI: 10.1016/j.bbagen.2004.06.021
38. Förster, T.; in: Sinanoglu (Ed.), O.; Modern Quantum Chemistry, Academic Press, New York, **1996**.
39. Cyril, L.; Earl, J. K.; Sperry, W. M.; *Biochemist's Handbook*, *E & FN Epon Led. Press, London*, **1961**.
40. S. Weiss, Fluorescence Spectroscopy of Single Biomolecules, *Science*, **1999**, *283*, 1676.
DOI: 10.1126/science.283.5408.1676
41. Valeur, B.; Molecular Fluorescence: Principles and Applications, Wiley, New York, **2001**.
ISBN: 3-527-60024-8
42. Kyhm K.; Kim, I.; Kang, M.; and Woo, H. Y.; *J. Nanosci. Nanotechnol*. **2012**, *12*, 7733.
DOI: 10.1166/jnn.2012.6633
43. Valeur, B.; Brochon, J. C.; New Trends in Fluorescence Spectroscopy, Springer Press, Berlin, **2001**.
44. Gao, W. H.; Li, N.; Chen, Y.W.; Xu, Y.; Lin, Y.; Yin, Y.; Hu, Z.; *J. Mol. Struct*., **2010**, *983*, 133.
DOI: 10.1016/j.molstruc.2010.08.042
45. Paal, K.; Shkarupin, A.; Beckford, L.; *Bioorg. Med. Chem*., **2007**, *15*, 1323.
DOI: 10.1016/j.bmc.2006.11.012

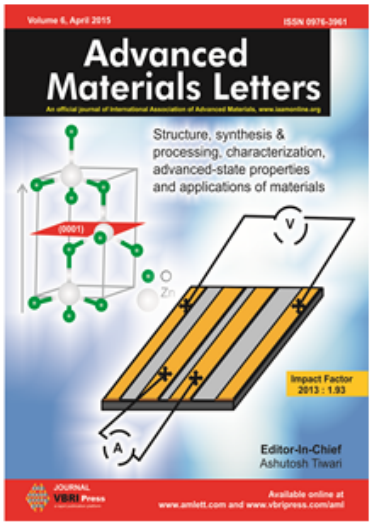

Supporting Information

Table 3. Thermodynamic parameters for the binding of STP with BSA at different temperatures.

Compound	Temperature (K)	ΔH (kJ/mol)	ΔS (J/mol/K)	ΔG (kJ/mol)
STP1	293	-168.28	-472.48	-27.84
STP2	293	-94.47	-235.28	-25.53
STP3	293	-79.36	-180.91	-26.35
STP4	293	-86.92	-202.03	-27.72
STP6	293	-60.46	-117.22	-26.12
STP1	303	-168.28	-472.48	-23.11
STP2	303	-94.47	-235.28	-23.18
STP3	303	-79.36	-180.91	-24.54
STP4	303	-86.92	-202.03	-25.70
STP6	303	-60.46	-117.22	-24.95
STP1	313	-168.28	-472.48	-18.39
STP2	313	-94.47	-235.28	-20.83
STP3	313	-79.36	-180.91	-22.73
STP4	313	-86.92	-202.03	-23.68
STP6	313	-60.46	-117.22	-23.77

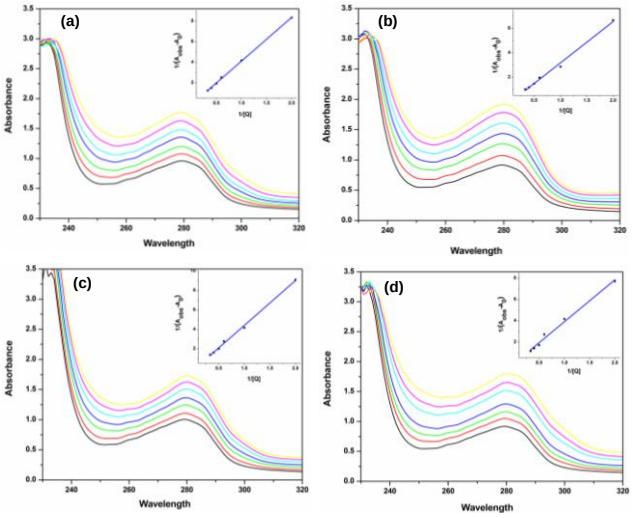

Supplementary Fig. 1. (color online) Absorption spectra of BSA (1 µM) in presence of STP2, STP3, STP4 and STP6 [a, b, c and d respectively] (1-7): (0 to 30 µM), inset showing calculation of K_{app} of BSA–STP complex; $1/(A_{obs}-A_0)$ versus 1/[STP] plot.

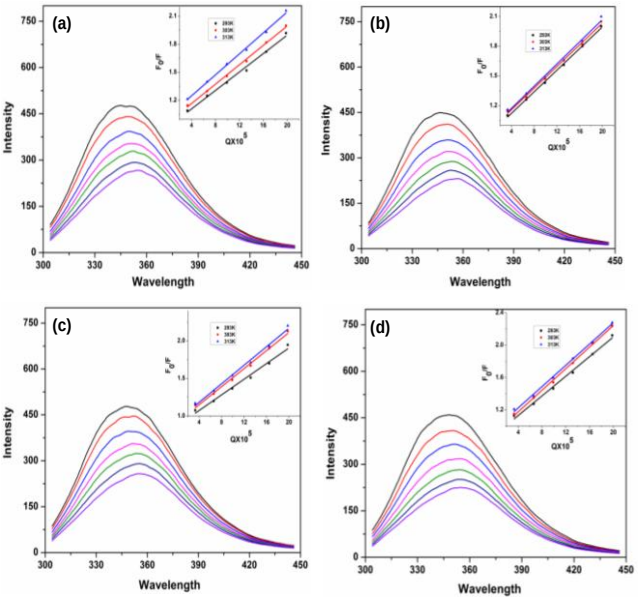

Supplementary Fig. 2. (color online) Fluorescence quenching spectra of BSA by STP2, STP3, STP4 and STP6 [a, b, c, and d respectively], λ_{ex}=279 nm; $C_{(BSA)}$= 1µM; $C_{(STP)}$ (1-7): (0 to 20 µM), inset showing Stern Volmer plot for STP2, STP3, STP4 and STP6 and BSA at 293, 303, and 313 K, respectively.

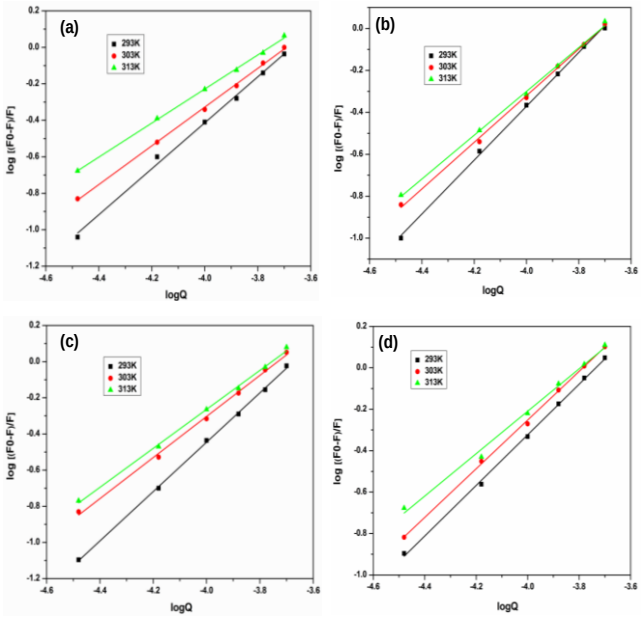

Supplementary Fig. 3. (color online) Plots of the STP2, STP3, STP4 and STP6 [a, b, c, and d respectively] quenching effect on BSA fluorescence at different temperature (293, 303, and 313 K).

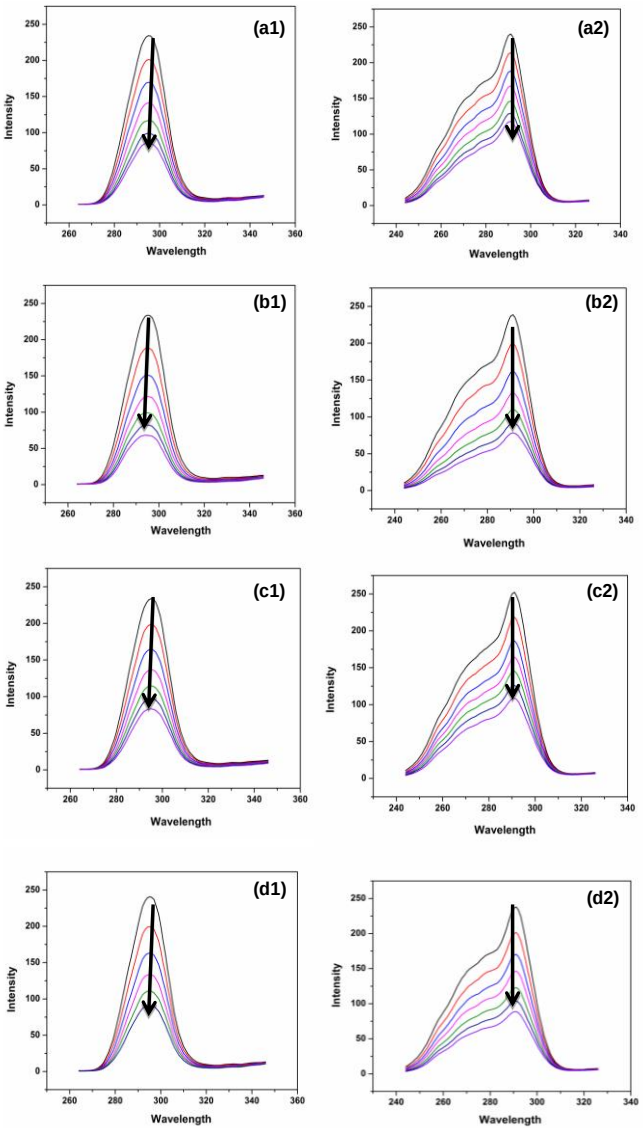

Fig. 5. (color online) Synchronous fluorescence spectra of BSA in presence of STP2, STP3, STP4 and STP6 [a, b, c, and d respectively] while the Δλ =15 nm (1) and Δλ=60nm (2).

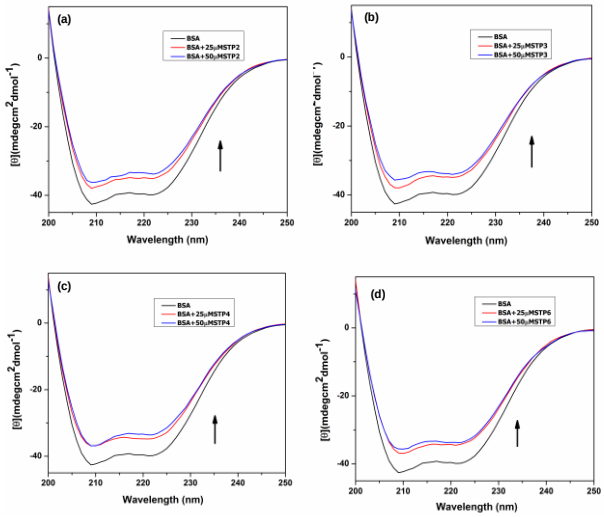

Fig. 6. (color online) UV-CD spectra of STP2, STP3, STP4 and STP6 [a, b, c, and d respectively] at the BSA concentration of 0.04 μM and SPT concentrations of 0 to 50μM.

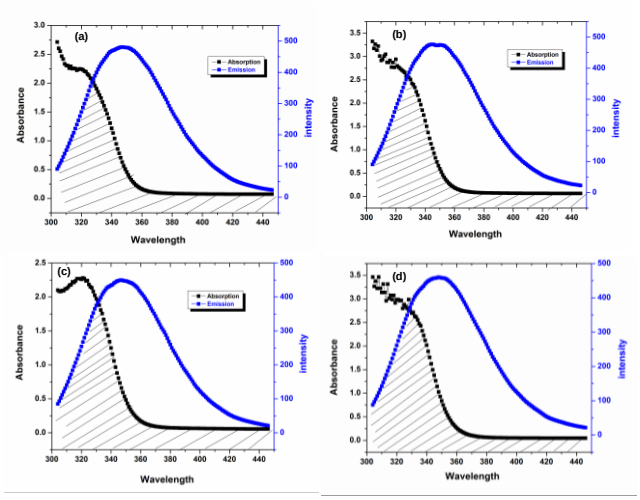

Fig. 7. (Color online) The overlap plot of the fluorescence emission spectra of BSA (1μM) and the UV absorption spectra of STP2, STP3, STP4 and STP6 (1 mM) [a, b, c, and d respectively].

Table 4. The energy transfer parameters between STP and BSA.

System	J cm^3·L/mol	E	R_0(nm)	r(nm)
BSA-STP1	2.74×10^{-15}	0.031	2.05	3.64
BSA-STP2	3.14×10^{-15}	0.086	2.10	3.12
BSA-STP3	2.92×10^{-15}	0.091	2.07	3.05
BSA-STP4	7.03×10^{-15}	0.071	2.40	3.69
BSA-STP6	4.43×10^{-15}	0.113	2.23	3.14